The Global Characteristics of the Wavenumber Spectrum of Ocean Surface Wind

YONGSHENG XU AND LEE-LUENG FU

Jet Propulsion Laboratory, California Institute of Technology, Pasadena, California

ROSS TULLOCH

Department of Earth, Atmospheric, and Planetary Sciences, Massachusetts Institute of Technology, Cambridge, Massachusetts

(Manuscript received 24 March 2011, in final form 14 May 2011)

ABSTRACT

The wavenumber spectra of wind kinetic energy over the ocean from Quick Scatterometer (QuikSCAT) observations have revealed complex spatial variability in the wavelength range of 1000–3000 km, with spectral slopes varying from −1.6 to −2.9. Here the authors performed a spectral analysis of QuikSCAT winds over the global ocean and found that (i) the spectral slopes become steeper toward the Poles in the Pacific and in the South Atlantic, and the slopes exhibit minimal longitudinal dependence in the South Pacific; (ii) the steepest slopes are in the tropical Indian Ocean and the shallowest slopes are in the tropical Pacific and Atlantic; and (iii) the spectra are steeper in winter than summer in most regions of the midlatitude Northern Hemisphere. The new findings reported in the paper provide a test bed for theoretical studies and atmospheric general circulation models.

1. Introduction

Fundamental questions of atmospheric and oceanic dynamics address the mechanisms underlying their equilibrium energy spectra and spectral energy transfers. Over the past five decades, large effort has been dedicated to characterizing the spatial variations of the spectrum of atmospheric kinetic energy, with a special interest in the extent to which it is compatible with spectral shapes predicted by theories. The atmospheric energy spectrum, in the wavelength range from a few kilometers to synoptic scales, was studied by Nastrom and Gage (1985). They analyzed wind and temperature data obtained from over 6000 commercial aircraft flights in the midlatitudes near the tropopause during the Global Atmospheric Sampling Program (GASP) and found that the wavenumber spectra have two different slopes. The spectra follow a −3 power law in the wavelength range of 1000–3000 km and a $-5/3$ power law in range of about 3–400 km.

The −3 spectral slope in the range of 1000–3000 km is typically interpreted as a forward enstrophy cascade and inverse energy cascade forced by the baroclinic instability acting at scales near the Rossby deformation wavelength, as predicted by Charney (1971). The interpretation of the $-5/3$ spectral slope at the higher wavenumbers is controversial. Charney's theory of geostrophic turbulence, which assumes potential vorticity (PV) driven dynamics in the interior and uniform temperature on the boundary, cannot explain the observed $-5/3$ slope. Explanations for the $-5/3$ slope in the literature fall into three general categories: (i) an inverse cascade of small-scale energy, produced perhaps by convection (Lilly 1989; Vallis et al. 1997); (ii) the production of gravity waves by unbalanced lows (Gardner et al. 1993; Koshyk et al. 1999); or (iii) a direct cascade of energy from the large scales (Tung and Orlando 2003; Lindborg 2005; Kitamura and Matsuda 2006; Tulloch and Smith 2009, hereafter TS09). Also note that the planetary boundary layer often contains energetic small-scale turbulence such as organized large eddies (rolls) with scales of order 1 km. However, it is not clear how such energy could affect scales of order 1000 km. As the quasigeostrophic (QG) forward enstrophy cascade proceeds downscale, if the Rossby number increases,

Corresponding author address: Yongsheng Xu, Jet Propulsion Laboratory, California Institute of Technology, 4800 Oak Grove Dr., Pasadena, CA 91109.
E-mail: yongsheng.xu@jpl.nasa.gov

DOI: 10.1175/JPO-D-11-059.1

there ought to be some scale where a breakdown of balance occurs, meaning that QG scaling no longer holds and highly stratified turbulence begins to dominate. In ''stratified turbulence,'' the energy spectrum has a $-5/3$ slope due to an ageostrophic forward energy cascade (Lindborg 2006), even when dominated by vortical motion (Waite and Bartello 2006). Waite and Bartello (2006) studied the transition from geostrophic to stratified turbulence through numerical simulations of forced rotating stratified turbulence. They found that the transition can occur when the Rossby number approaches 0.4 or larger.

As a counterpoint to Charney's QG turbulence theory, Blumen (1978) proposed the theory of surface QG (SQG) turbulence, which assumes temperature-driven turbulence on the boundary with uniform PV in the interior (see also Held et al. 1995). In SQG, a $-5/3$ kinetic energy spectrum is predicted as a result of a forward potential energy cascade at the surface and conversion from potential energy to kinetic energy (Capet et al. 2008). Since SQG cannot explain the observed -3 slope, Tulloch and Smith (2006), hereafter TS06), proposed a finite-depth surface quasigeostrophic (fSQG) turbulence theory, which takes into account the barotropization of temperature anomalies at large horizontal scales, leading to a transition scale between -3 and $-5/3$ spectral slopes. The transition between spectral slopes in fSQG depends on both latitude and the thickness of the fluid and occurs at a horizontal wavenumber $k_{\text{trans}} \sim f/NH$, where f is the Coriolis parameter, N is stratification, and H is the thickness of the fluid. In a follow up paper, TS09 proposed a model, driven by a baroclinically unstable mean zonal flow, which explicitly couples interior PV dynamics with boundary temperature dynamics. In their model the resulting kinetic energy spectrum at the surface is the superposition of competing forward cascades: a steep k^{-3} interior PV driven enstrophy cascade and a shallow $k^{-5/3}$ surface temperature-driven energy cascade. TS09 derived a transition scale k_{trans} that depends on the relative strengths of the energy and enstrophy spectral fluxes [see their Eqs. (19)–(20)]. In the f-plane limit, the resulting k_{trans} again scales with f/NH, plus a shear-dependent term (see Klein et al. 2010, for an independent derivation of k_{trans}).

Satellite scatterometers measure wind velocity near the ocean surface. Early investigations of wind spectra with satellite scatterometer observations focused on a few regions in the Pacific Ocean (Freilich and Chelton 1986; Wikle et al. 1999; Patoux and Brown 2001). These studies reported spectral slopes from -1.67 to -2.6 for wavelengths of ~50–2000 km. From these studies it is difficult to draw conclusions on the prevalence of either a $-5/3$ or -3 power law. Moreover, shot noise in the satellite wind direction field can affect spectral slopes below 300 km where the $-5/3$ slope is expected (E. Rodriguez 2011, personal communication). The slope estimation may be contaminated at wavelengths below 300 km. In this paper, we focus on the QG inertial range where both measurements and theoretical interpretation are less controversial to evaluate the geographic pattern of spectral slope and its consistency with existing theories. Here we construct the first global map showing the variability of the wind kinetic energy spectrum in the range from 1000 to 3000 km where geostrophic turbulence scaling applies. The seasonal variation of the spectrum is also discussed.

2. Data and methodology

The Quick Scatterometer (QuikSCAT) is a polar-orbiting satellite that provided estimates of wind speed and direction over the oceans from 1999 to 2009 (Chelton et al. 2004). QuikSCAT sampled more than 90% of the ocean every 24 h. We used the QuikSCAT L2B 25-km swath wind observations over 2 yr from January 2007 to December 2008. The data is from the official dataset (which covers period from 1999 to 2009) produced by the QuikSCAT Project through the SeaWinds Processing and Analysis Center (Dunbar et al. 2006). The QuikSCAT data are quite voluminous over swaths of thousands of kilometers wide. It takes about 5-day computing time for a 1-yr global survey (see method description in the next paragraph). After extensive testing on regional basis, we found that the slope difference between using 2-yr (2007–08) and 10-yr (1999–2009) QuikSCAT data is generally smaller than 0.06, and the seasonal slope difference is generally smaller than 0.1. Therefore, we used 2-yr QuikSCAT data and believe that the differences do not affect the major conclusions of the paper. The SeaWinds instrument on the QuikSCAT satellite uses a rotating dish antenna with two spot beams, which, after processing of the backscatter data, provide wind measurements on a 1800-km-wide swath centered on the satellite's nadir subtrack, with a 25-km resolution. Each swath can then be represented on 25-km ''grids,'' slightly inclined with respect to the north–south axis.

The time mean was removed from the wind data to obtain wind velocity anomalies. The time mean was calculated at each point along the artificial meridional lines for the investigated period. We computed the eddy kinetic energy (EKE) spectra at points on a $3° \times 3°$ grid for the global ocean between 60°S and 60°N. To calculate the spectrum for each grid point, we assigned artificial ground-track-like lines within a $44° \times 18°$ degree box centered at that grid point. The lines are along

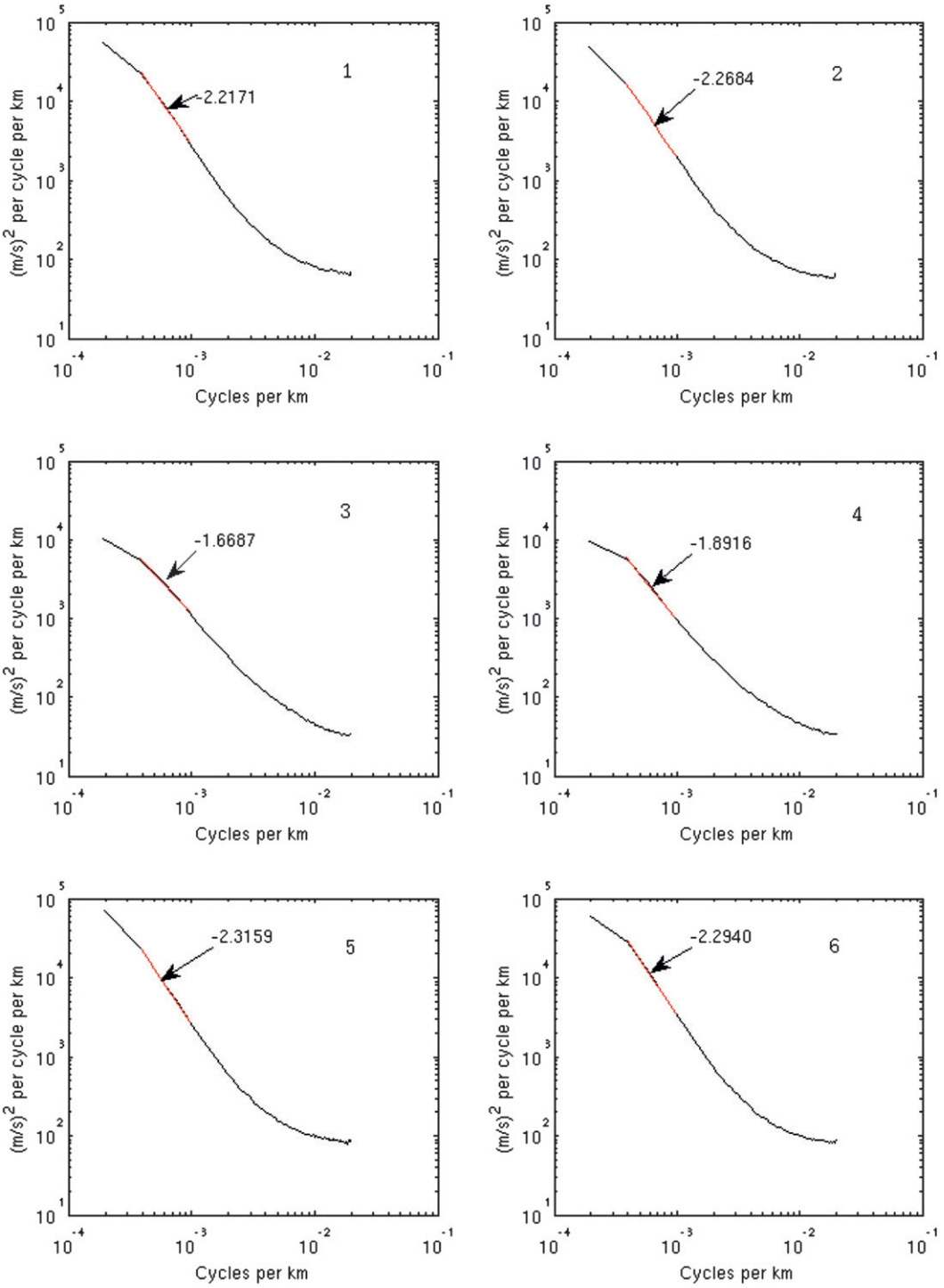

FIG. 1. EKE spectra at six typical regions. The positions of the plots were shown as the numbered squares in Fig. 2.

QuikSCAT ascending and/or descending swath directions. The interval between parallel lines is 3°, and the sampling interval along the lines is 25 km. The value of each data point along a line was obtained by searching for the nearest wind velocity anomaly within a distance of 25 km. In a 44° × 18° degree box, the missing data due to ice, land, and bad measurements are flagged as bad data, and we used only the lines that are longer than 3000 km and have 90% or more good data. The gaps were filled by linear interpolation.

The EKE spectrum was obtained by averaging the zonal and meridional velocity power spectra calculated along all eligible lines within the box. The spectral slope in the wavelength range of 1000–3000 km was calculated as the value at that grid point. The QuikSCAT measurements poleward of 65°S and 73°N were not used in the calculation to avoid extensive sea ice coverage. For a grid point near coastal or polar regions, large amounts of data within its 44° × 18° degree box can be missed due to land or ice. The slope at that grid point was still calculated using all eligible lines within the box and thus may be biased toward the open-ocean values. There are typically eight eligible lines in the open ocean in a box, while the amount of the eligible lines can be reduced to one in certain coastal regions. However, even in these regions there are ~700 repeats during the 2-year period. Figure 1 shows the EKE spectra at six typical regions. The curvature and flattening of the spectra below about 400 km is likely due to shot noise in the wind direction measurements as noted earlier. These results, in particular in the Pacific Ocean (left column), are consistent with the previous studies (Freilich and Chelton 1986; Patoux and Brown 2001).

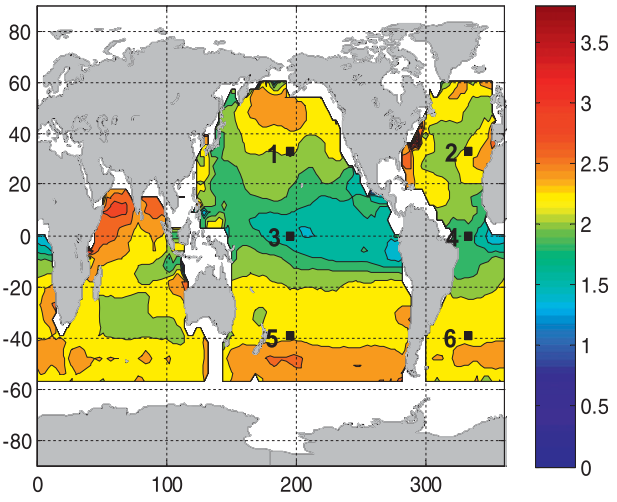

FIG. 2. The global distribution of the spectral slopes of kinetic wavenumber spectrum in the wavelength band of 1000–3000 km estimated from the QuikSCAT scatterometer measurements. The sign of the slopes was reversed to make the value positive.

3. Results and analyses

Figure 2 shows the geographic variability of the atmospheric EKE wavenumber spectral slopes in the wavelength range of 1000–3000 km. It can be seen that the spectral slope takes on a wide range of values from −1.6 to −2.9, which is roughly between $-5/3$ and −3. The result is quite different from that predicted by the QG turbulence theory in which a power law with an approximate −3 slope governs the synoptic scales. Charney's geostrophic turbulence theory was based on a large-scale flow that was not appreciably influenced by boundary constraints. He also pointed out that baroclinic instability and frontogenesis, associated with surface temperature gradients, could alter the k^{-3} spectrum, although he did not conduct an analysis of such effects on the spectrum. Figure 2 is probably an indicator of large boundary influence on the k^{-3} spectrum. The TS06 and TS09 studies incorporated the boundary effect in a way that led to a transition between two dominant spectral slopes. This transition scale depends on the latitude. Consequently, the spectral slope in a certain range of spatial scales can change from $-5/3$ to −3, depending on the regional transition wavenumber k_{trans}.

a. Latitudinal dependence

The prominent feature of Fig. 2 is that the spectral slope steepens poleward in vast areas of the Pacific Ocean. Similar features also prevail in the South Atlantic Ocean. In particular, the contours of the spectral slope in the South Pacific are nearly parallel to latitude lines, showing little longitudinal dependence. Neither QG nor SQG can explain this latitudinal dependence on its own. The transition theories proposed by TS06 and TS09 may have some relevance to the latitude dependence since the spectral slope can vary between $-5/3$ and −3, depending on whether the transition scale is below, or within the investigated wavelength range. According to TS09, the transition occurs at about 500 km in the midlatitudes, which is smaller than the 1000–3000-km range. It might explain the steep −2.6 slope in the Southern Ocean and the North Pacific. At lower latitudes, f decreases and H (which is the depth of the troposphere) increases and the transition can occurs within the 1000–3000-km range. Therefore, the spectral slope is expected to become shallower toward the equator as a result of the increasing ageostrophic contributions. Furthermore, stratification plays an important role to constrain turbulence motion when f is small near the equator (Waite and Bartello 2006). The Rossby number for motions at wavelength range of 1000–3000 km becomes large in the tropics, so the stratified turbulence theory may explain the shallow slopes (i.e., regions of light blue) in the tropical Pacific and Atlantic. Another point is that the synoptic baroclinic instability forces the QG turbulence in the midlatitudes, while convective motions dominate in the tropics. This is another factor for the different spectral slopes in the two regions (Patoux and Brown 2001).

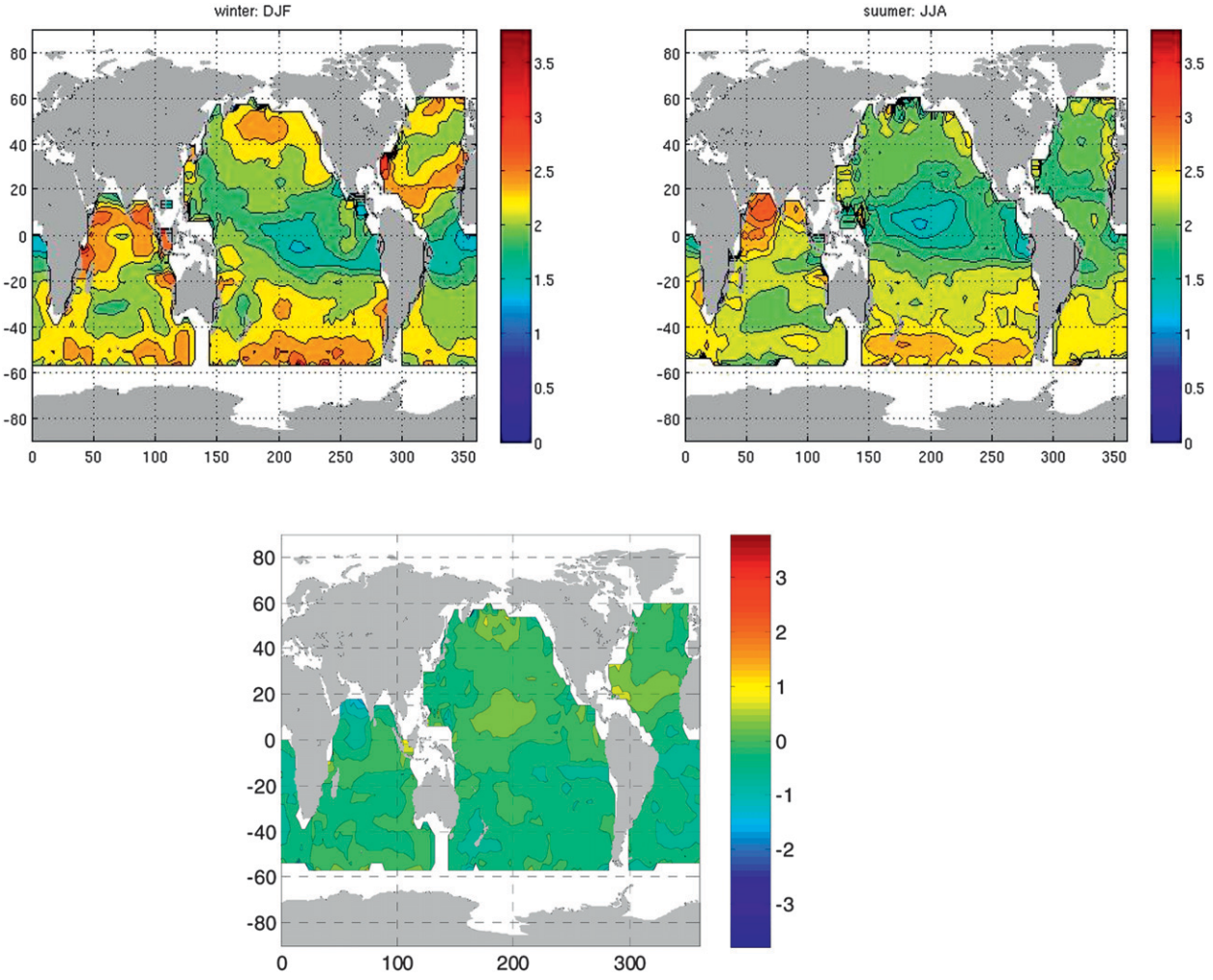

FIG. 3. The global distribution of the spectral slopes of kinetic wavenumber spectrum in the wavelength band of 1000–3000 km estimated from the QuikSCAT scatterometer measurements (the sign of the slopes was reversed to make the value positive). (top left) The spectral slopes of boreal winter (December, January, and February) and (top right) the spectral slopes of boreal summer (June, July, and August). (bottom) The subtraction of the spectral slopes of summer from the winter.

b. Different features in the three major oceans

Figure 2 reveals significant differences in spectral slope in the three major oceans. In contrast to the Pacific and the South Atlantic, where spectral slope is primarily latitudinally dependent, the spectral slopes in the North Atlantic and the South Indian Ocean exhibit more complex patterns and do not exhibit a clear latitudinal dependence. The steepest slopes (approximately −2.5 to −2.9) occur in the tropical Indian Ocean, while the tropical Pacific and Atlantic Oceans are characterized by shallow slopes (approximately −1.5 to −2). This sharp contrast is likely a reflection of the very different dynamic regimes in these regions. The wind circulation in the tropical Indian Ocean is controlled by a monsoon system that is driven by horizontal differential heating between land and ocean. The tropical Pacific and Atlantic Oceans, especially the intertropical convergence zone (ITCZ), are characterized by convective activity driven by solar heating. These very different regional dynamics are likely to have a strong influence on the spectral slope of the EKE spectrum. Figure 2 also implies a profound influence of land on atmospheric dynamics over the ocean. The spectral slope contours are mainly dependent on latitude in the Southern Hemisphere where there is not much land, while in the Northern Hemisphere they exhibit more longitudinal dependence, reflecting the influence of land–sea boundaries. Compared to the ocean, the land has smaller heat content and exhibits more rapid atmospheric heating

(and cooling). The signals from the land can be carried by atmospheric general circulation and have a far-reaching impact on atmospheric dynamics over the ocean.

c. Seasonal differences

Spectral slopes and their differences are shown for winter and summer in Fig. 3. The spectrum is shallower in summer than in winter in most regions of the midlatitude Northern Hemisphere. The slope changes in the Southern Ocean are relatively small, especially in the South Atlantic. The slope variations in the tropics are even weaker than in the midlatitudes. The seasonality of the slope is likely related to the strength of the baroclinic activity at synoptic scales. Baroclinic excitation peaks in winter in the midlatitude Northern Hemisphere (Nastrom and Gage 1985), while the strength of atmospheric activity does not vary as much throughout the year in the Southern Ocean, and the variations are much weaker in tropical regions (Patoux and Brown 2001). It is interesting to compare Fig. 3 with the seasonal map of wind power distribution as shown in Fig. 1 of Liu et al. (2008). There is a larger wind power in the midlatitude Northern Hemisphere in boreal winter than summer, in agreement with the seasonality of the baroclinic activity. It is interesting to note that the seasonality of the spectral slope is much weaker in the Southern Ocean where the seasonal difference in the wind energy is also weaker, as shown in Liu et al. (2008). However, it is also worth pointing out that the slope is steeper in some regions of the Southern Ocean in summer than winter, which cannot be explained by the baroclinic argument.

4. Summary and discussion

We constructed a global map of the slope of the wavenumber spectrum of atmospheric kinetic energy from the QuikSCAT satellite wind observations for the period 2007–08. The map reveals a complex geographic pattern of variability in the 1000–3000-km wavelength range, where a -3 power-law relationship is expected from the geostrophic turbulence theory. The slope of the spectra shows a strong latitudinal dependence in the midlatitudes. This result is interpreted to be caused by the latitudinal variation of the transition wavenumber k_{trans}, as defined by TS09 to separate two spectral regimes. The shallow slope in the tropical Pacific and the tropical Atlantic Oceans may be explained by the stratified turbulence theory of Waite and Bartello (2006). The map also reveals many regional features, such as the distinct slope patterns in the Indian Ocean and the North Atlantic, which poses challenges for further theoretical studies.

The pattern of the slope variability is apparently related to the energy levels of regional baroclinic activity. Charney's geostrophic turbulence theory assumes that energy is input via synoptic baroclinic excitation. The synoptic baroclinic activity is most significant in the midlatitude (40°–60°), and therefore, the slope is closer to -3 there. The dependence on baroclinic activity is also suggested by the spectral slope's seasonal dependence.

In the tropical regions of the Pacific and Atlantic, more energy is introduced at the convection scale (i.e., higher wavenumbers) and large-scale baroclinic activity is relatively weak, leading to shallower spectral slopes. There is evidence that the Indian monsoon is marked by distinct baroclinic activity (Krishnakumar et al. 1992; Xu and Guoxiong1999), which might explain the steeper spectra observed in the Indian Ocean, as compared to the rest of the tropics.

Acknowledgments. The research presented in the paper was carried out at the Jet Propulsion Laboratory, California Institute of Technology, under contract with the National Aeronautics and Space Administration. The authors thank Ernesto Rodriguez, Jerome Patoux, Shafer Smith, Peter Bartello, Yuji Kitamura, and Erik Lindborg for their comments. Government sponsorship acknowledged.

REFERENCES

Blumen, W., 1978: Uniform potential vorticity flow: Part I. Theory of wave interactions and two-dimensional turbulence. *J. Atmos. Sci.,* **35,** 774–783.

Capet, X., P. Klein, B. L. Hua, G. Lapeyre, and J. C. McWilliams, 2008: Surface kinetic energy transfer in surface quasigeostrophic flows. *J. Fluid Mech.,* **604,** 165–174.

Charney, J. G., 1971: Geostrophic turbulence. *J. Atmos. Sci.,* **28,** 1087–1095.

Chelton, D. B., M. G. Schlax, M. H. Freilich, and R. F. Milliff, 2004: Satellite measurements reveal persistent small-scale features in ocean winds. *Science,* **303,** 978–983.

Dunbar, R. S., and Coauthors, 2006: QuikSCAT science data product user manual, Version 3.0. JPL Document D-18053–Rev. A, Jet Propulsion Laboratory, Pasadena, CA, 85 pp.

Freilich, M. H., and D. B. Chelton, 1986: Wavenumber spectra of Pacific winds measured by the SEASAT scatterometer. *J. Phys. Oceanogr.,* **16,** 741–757.

Gardner, C. S., C. A. Hostetler, and S. Lintelman, 1993: Influence of the mean wind field on the separability of atmospheric perturbation spectra. *J. Geophys. Res.,* **98,** 8859–8872.

Held, I. M., R. T. Pierrehumbert, S. T. Garner, and K. L. Swanson, 1995: Surface quasigeostrophic dynamics. *J. Fluid Mech.,* **282,** 1–20.

Kitamura, Y., and Y. Matsuda, 2006: The kh-3 and kh-5/3 energy spectra in stratified turbulence. *Geophys. Res. Lett.,* **33,** L05809, doi:10.1029/2005GL024996.

Klein, P., G. Lapeyre, G. Roullet, S. Le Gentil, and H. Sasaki, 2010: Ocean turbulence at meso and submesoscales: Connection between surface and interior dynamics. *Geophys. Astrophys. Fluid Dyn.,* **104,** 421–437, doi:10.1080/03091929.2010.532498.

Koshyk, J. N., K. Hamilton, and J. D. Mahlman, 1999: Simulation of the k-5/3 mesoscale spectral regime in the GFDL SKYHI

middle atmosphere general circulation model. *Geophys. Res. Lett.,* **26,** 843–846.

Krishnakumar, V., R. N. Keshavamurty, and S. V. Kasture, 1992: Moist baroclinic instability and the growth of monsoon depressions — Linear and nonlinear studies. *Proc. Indiana Acad. Sci.,* **101,** 123–152.

Lilly, D. K., 1989: Two-dimensional turbulence generated by energy sources at two scales. *J. Atmos. Sci.,* **46,** 2026–2030.

Lindborg, E., 2005: The effect of rotation on the mesoscale energy cascade in the free atmosphere. *Geophys. Res. Lett.,* **32,** L01809, doi:10.1029/2004GL021319.

——, 2006: The energy cascade in a strongly stratified fluid. *J. Fluid Mech.,* **550,** 207–242.

Liu, W. T., W. Tang, and X. Xie, 2008: Wind power distribution over the ocean. *Geophys. Res. Lett.,* **35,** L13808, doi:10.1029/2008GL034172.

Nastrom, G. D., and K. S. Gage, 1985: A climatology of atmospheric wavenumber spectra of wind and temperature observed by commercial aircraft. *J. Atmos. Sci.,* **42,** 950–960.

Patoux, J., and R. A. Brown, 2001: Spectral analysis of QuikSCAT surface winds and two-dimensional turbulence. *J. Geophys. Res.,* **106,** 23 995–24 005.

Tulloch, R. T., and K. S. Smith, 2006: A theory for the atmospheric energy spectrum: Depth-limited temperature anomalies at the tropopause. *Proc. Natl. Acad. Sci.,* **103** (40), 14 690–14 694.

——, and ——, 2009: Quasigeostrophic turbulence with explicit surface dynamics: Application to the atmospheric energy spectrum. *J. Atmos. Sci.,* **66,** 450–467.

Tung, K. K., and W. W. Orlando, 2003: The k-3 and k-5/3 energy spectrum of atmospheric turbulence: Quasigeostrophic two-level model simulation. *J. Atmos. Sci.,* **60,** 824–835.

Vallis, G. K., G. J. Shutts, and M. E. B. Gray, 1997: Balanced mesoscale motion and stratified turbulence forced by convection. *Quart. J. Roy. Meteor. Soc.,* **123,** 1621–1652.

Waite, M. L., and P. Bartello, 2006: The transition from geostrophic to stratified turbulence. *J. Fluid Mech.,* **568,** 89–108.

Wikle, C. K., R. F. Milliff, and W. G. Large, 1999: Surface wind variability on spatial scales from 1 to 1000 km observed during TOGA COARE. *J. Atmos. Sci.,* **56,** 2222–2231.

Xu, J., and W. Guoxiong, 1999: Dynamic features and maintenance mechanism of the Asian summer monsoon subsystem. *Adv. Atmos. Sci.,* **16** (4), 523–536.